

Gas Permeation Behavior of Pebax-1657 Nanocomposite Membrane Incorporated with Multiwalled Carbon Nanotubes

R. Surya Murali,[†] S. Sridhar,^{*,‡} T. Sankarshana,[‡] and Y. V. L. Ravikumar[†]

Membrane Separations Group, Chemical Engineering Division, Indian Institute of Chemical Technology, Hyderabad 500 007, India, and College of Technology, Osmania University, Hyderabad 500 007, India

Incorporation of multiwalled carbon nanotubes (MWNT) on the gas permeation properties of H₂, CO₂, O₂, and N₂ gases in poly(ether-*block*-amide) (Pebax-1657) membrane has been investigated. Pebax-1657 was dissolved in the ethanol–water mixture and cast on an ultraporous polyethersulfone substrate followed by complete solvent evaporation. Nanocomposite membranes were prepared by dispersion of MWNT in concentrations of 0–5% of polymer weight in the Pebax solutions with sonication for 2 h to ensure uniformity. Cross-linking was carried out in hexane medium using 2,4-toluylene diisocyanate (TDI). The permeabilities of pure gases were measured at room temperature, and the ideal selectivities were determined at pressures varying from 1–3 MPa using an indigenously built high-pressure gas separation manifold. For neat Pebax membrane, high permeabilities of 55.8 and 32.1 barrers were observed for CO₂ and H₂ gases, respectively, whereas that of N₂ was as low as 1.4 barrers. The selectivity of cross-linked 2% MWNT Pebax membrane was enhanced from 83.2 to 162 with increasing feed pressure (1–3 MPa) for the CO₂/N₂ gas pair, whereas the corresponding values for H₂/N₂ and O₂/N₂ systems were found to be in the range 82.5–90 and 7.1–6.8, respectively. The membranes were characterized by scanning electron microscopy (SEM) to study surface and cross-sectional morphologies. Fourier transform infrared (FT-IR), wide-angle X-ray diffraction (WAXD), and ion exchange capacity (IEC) studies were carried out to determine the effect of MWNT incorporation on intermolecular interactions, degree of crystallinity, and extent of cross-linking, respectively. Fractional free volume (FFV) calculations based on density measurements were conducted along with water sorption studies to explain permeation behavior. The use of modified block copolymer membranes provides a means for separation of CO₂ from N₂ in power plants, H₂ recycle from ammonia purge gas, O₂ enrichment from air for medical applications, and CO₂ removal from water-gas shift reaction to improve H₂ yield.

1. Introduction

Gas separation through polymer membranes is considered to be an effective tool for the separation of gaseous mixtures due to high separation efficiency, low running costs, and simple operating procedures compared to conventional separation methods.^{1–3} Polymeric membranes generally undergo a trade-off limitation between permeability and selectivity as shown in the upper bound curves developed by Robeson.⁴ Attempts are being made to improve the performance by modifying the polymer both physically and chemically to bring about an increase in both flux and selectivity of the membrane. Literature reveals that physical modifications have been done through incorporation of fillers into the polymer matrix like carbon nanotubes, zeolites, silica, alumina, carbon molecular sieves, and other inorganics.^{5–10} Polymer membranes have also been chemically modified by grafting and cross-linking, which alter the structure and properties.^{11–14} Hydrogen is the fuel of the future and therefore its conservation/recovery attains great significance, globally. The separation of H₂ from N₂ is critical in the context of the recovery of hydrogen from ammonia purge gas. Air separation is a challenging problem due to the similar physical properties and molecular sizes of O₂ and N₂. Enriched O₂ is widely used in medical and welding applications whereas pure N₂ is an economical option for creation of inert atmospheres. Isolation of CO₂ from emission sources such as power plants and chemical industries is an important task to minimize

global warming. Coal fired power plant flue gas streams are rich in CO₂ and N₂. Several processes like adsorption, absorption, cryogenic fractionation, and membrane technology are available for CO₂ capture. In the last several years, dynamic developments in membrane technology for CO₂/N₂ separation have occurred. Captured CO₂ was sent to the sequestration process and CO₂ lean stream to the atmosphere. Another application is the water-gas shift reaction wherein hydrogen is produced along with CO₂ in the product upon catalytic reaction of CO with water. Membranes can be used to separate the CO₂ from the product stream to enrich hydrogen.

Rigid polyamides have attracted much attention as the basic material for preparing gas separation membranes due to their glassy but selective nature. In contrast, polyethers are rubbery polymers containing large free volume owing to their flexible chains and the presence of voids between them. Poly(ether-*block*-amide) resin is best known under the trademark Pebax and is a thermoplastic elastomer combining linear chains of the hard polyamide segments that provide mechanical strength with interspacing of flexible polyether segments which offer high permeability due to greater chain mobility of the ether linkage.^{15,16} Different grades of Pebax have been prepared by varying ether and amide compositions for gas transport applications.^{17–19} In the present work, Pebax-1657, which is constituted by 40% amide groups and 60% ether linkages, was selected as the base polymer for modification.

Carbon nanotubes (CNTs) have been considered to be potential fillers for mixed matrix membranes due to their outstanding mechanical, thermal, and electrical properties.⁵ CNTs are composed entirely of sp² hybridization bonds, similar to those of graphite and this bonding structure, stronger than

* To whom correspondence should be addressed. Tel.: +91-40-27191394. Fax: +91-40-27193626. E-mail: sridhar11in@yahoo.com.

[†] Indian Institute of Chemical Technology.

[‡] Osmania University.

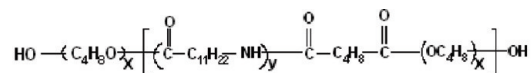
the sp^3 bonds found in diamond, provides the molecules with their unique mechanical strength and thermal stability. Therefore small concentrations of CNTs could substantially improve mechanical strength of polymer membranes. Moreover, CNTs are also conductive fillers and contribute to the electrical properties of the polymer matrix.²⁰ Gas permeation rates in CNTs were found to be several orders of magnitude faster than in other inorganic fillers such as zeolites owing to the inherent smoothness of nanotubes. If used as membranes CNTs could exhibit flux/selectivity characteristics far exceeding any other inorganic materials by increasing the diffusivity.⁵ CNTs have been used to improve properties of several polymeric materials.^{20–26} Cong. et al.²⁰ reported a CO_2 permeability of 148 barrers at 5% MWNT concentration. Polycarbonate loaded with single walled (SWNT) and multiwalled (MWNT) carbon nanotubes appeared to have potential for H_2 separation.²⁵ Hinds et al.²⁶ reported MWNT loaded membranes to have potential applications in chemical separations and sensors. They also found SWNT to disperse more uniformly in the polymer after functionalization with carboxylic acid.

A literature survey reveals the absence of any previous study on gas permeation properties of MWNT loaded Pebax-1657, which forms the focus of this investigation. The authors had earlier reported performance of cross-linked Pebax 2533 membrane for CO_2/CH_4 separation.²⁷ In the present work, Pebax membranes were filled with MWNT and cross-linked by TDI to study permeation of pure H_2 , O_2 , N_2 , and CO_2 gases. The extent of loading on the morphological structure and separation performance of the membrane was evaluated.

2. Experimental Section

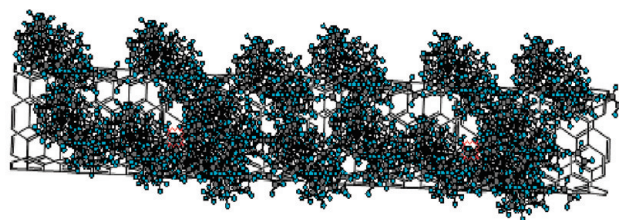
2.1. Materials. Pebax-1657 was purchased from Atofina Chemicals, France. Multiwalled carbon nanotubes (MWNT) of diameter 10–20 nm, length 5–15 μm , and surface area 116 m^2/g were supplied by Permionics Membranes Pvt. Ltd., Vadodara, India. 2,4-Toluylene diisocyanate (TDI) and ethanol were supplied by Loba Chemie, Mumbai, India, whereas polyethersulfone (PES) powder was procured from Radel, USA. Cylinders of pure CO_2 , H_2 , O_2 , and N_2 were supplied by BOC Gases Ltd., Hyderabad, India. Deionized water was produced with a laboratory reverse osmosis system.

2.2. Membrane Preparation. **2.2.1. Preparation of Pebax Membrane.** The structure and composition of Pebax is shown in Figure 1a. It is composed of 40% amide block and 60% ether block. PES substrate of approximately 30 000 molecular weight cutoff (MWCO) was prepared by the phase inversion method. An 18% w/v solution of PES in dimethyl formamide solvent containing 3% propionic acid as an additive was cast on a nonwoven polyester fabric which was affixed on a glass plate. After casting, the glass plate was immediately immersed in an ice-cold water bath for 5 min to obtain a 45–50 μm thick ultraporous PES substrate. The substrate was characterized using a 0.2% w/v standard solution of polyethylene glycol (PEG). Pebax composite membranes were then prepared on the PES substrate by the solution casting and solvent evaporation technique. A 4 wt % solution was prepared by adding Pebax-1657 grade pellets to a solvent mixture of 70% ethanol and 30% v/v water. The polymer was dissolved at 90 $^{\circ}C$ with vigorous stirring over a 6 h period. The 4 wt % polymer concentration was decided on the basis of viscosity considerations. The bubble free solution was cast on the PES substrate to the desired thickness using a doctor's blade. The membrane was dried at ambient temperature (30 $^{\circ}C$) for 3 h and

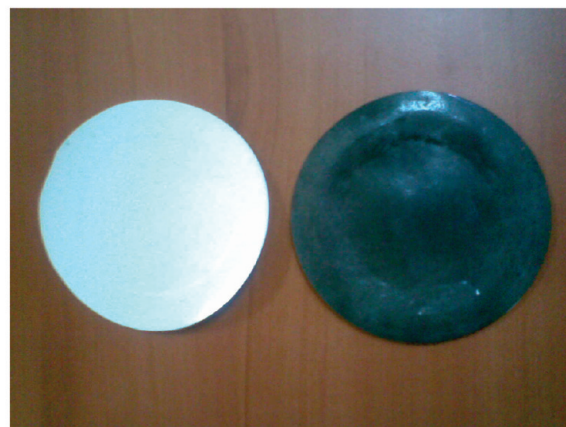


where $y=0.4$, $x=0.6$

(a)



(b)



(c)

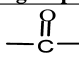
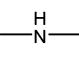
Figure 1. (a) Structure of Pebax, (b) hypothetical view of polymer matrix showing MWNT surrounded by Pebax chains, and (c) photograph of Pebax and MWNT-Pebax membranes.

subsequently in a vacuum oven at 60 $^{\circ}C$ followed by vacuum drying for 24 h to remove any residual solvent.

2.2.2. Preparation of MWNT Loaded Pebax Membrane. Li et al.²⁸ describes some of the standard techniques for the preparation of nanocomposite membranes. In the present work, the solution blending technique was adopted to fabricate polymer–inorganic nanocomposite membranes. MWNT in proportions of 2 and 5 wt % of the polymer weight were added to the 4% Pebax polymer solution and kept under constant stirring at 60–70 $^{\circ}C$ for 20 h to uniformly disperse the nanotubes and subsequently subjected to sonication for 3 h. Figure 1b shows a hypothetical view of MWNT surrounded by polymer chains. The bubble free solution was cast on PES substrate following the same procedure described earlier. The dispersion of carbon nanotubes in the Pebax solution was observed to be uniform. After the sonication step there was no settling down of the MWNT during the membrane casting and solvent evaporation steps. Figure 1c shows the pictures of pristine Pebax (white) and MWNT-Pebax (black) membranes. The consistent black coloration visible in the picture of the MWNT-Pebax membrane reveals a uniform dispersion of MWNT on the membrane surface.

2.2.3. Preparation of Cross-Linked Pebax Membrane. Cross-linking of Pebax and MWNT loaded Pebax membranes were done by the procedure described elsewhere.²⁷ Membranes were immersed in a 2% (v/v) solution of TDI in hexane for 20 h. Cross-linked membranes were rinsed with distilled water

Table 1. van der Waal's Volume and Molar Volume of Chemical Groups Constituting the Pebax Polymer

Chemical group	M _w (g/mol)	v _w (cm ³ /mol)
	28.01	11.7
—CH ₂ —	14.03	10.23
	15.02	4.0
—O—	16.0	5.5

for 1 h followed by drying in a vacuum oven at 60 °C for 24 h. Throughout this manuscript, cross-linked Pebax is denoted as X-Pebax, MWNT incorporated Pebax as MWNT-Pebax, and membranes with both the modifications as MWNT-X-Pebax.

2.3. Membrane Characterization. **2.3.1. WAXD.** A Siemens D 5000 powder X-ray diffractometer was used to study the solid-state morphology of Pebax and MWNT-Pebax nanocomposite membranes. X-rays of 1.5406 Å wavelengths were generated by a CuK-α source. The angle (2θ) of diffraction was varied from 0° to 65° to identify the crystal structure and intermolecular distances between the intersegmental chains.

2.3.2. FTIR. FTIR spectra of MWNT, Pebax, X-Pebax, and MWNT-Pebax nanocomposite were scanned between 4000 and 400 cm⁻¹ using a Perkin-Elmer-283B FTIR spectrometer.

2.3.3. SEM. The surface and cross-sectional morphologies of MWNT, Pebax, and the nanocomposite were examined by scanning electron microscopy (SEM) using a Hitachi S2150 microscope. Before characterization of the cross-section, the samples were cut in liquid nitrogen medium.

2.3.4. Measurement of Density by the Flotation Method. The polymer film density was measured by the flotation method in a mixture of CaNO₃ (2.5 g/cm³) and water (1.0 g/cm³).²⁹ A piece of Pebax membrane was placed in a beaker to which 10 mL of water was added. Since the membrane density was greater than water, it sunk to the bottom of the beaker. CaNO₃ salt was then added slowly with constant stirring of the solution to increase its density. At a certain point of addition, the membrane started to move upward and attain a position of floating where it neither sunk nor reached the surface of the solution indicating that the solution and membrane densities were equal. The density of the solution was then measured by a density meter at 30 °C. The same procedure was repeated for MWNT-Pebax membranes.

2.3.5. Determination of Fractional Free Volume (FFV), Ion Exchange Capacity (IEC), and Water Sorption. The fractional free volume (FFV) of the membranes was determined from³⁰

$$\text{FFV} = 1 - 1.3v_w\rho$$

where ρ represents the density of the neat or nanocomposite membrane and v_w is the van der Waal's volume of the repeat unit of Pebax in cubic centimeters/gram, which was calculated using the group contribution method of Bondi³¹ considering only the amide $[\text{CO}-(\text{CH}_2)_{11}-\text{NH}]$ and ether $[\text{O}(\text{CH}_2)_4]$ segments in the structure of Pebax-1657 shown in Figure 1a. Table 1 lists van der Waal's volumes (cubic centimeters/mole) and molecular weight (grams/mole) of different groups constituting the repeat unit of Pebax.³² Molecular weight (M_w) of the repeat unit was found to be 122.2 g/mol and the van der Waal's volume 79.14 cc/mol assuming 40% amide and 60% ether

Table 2. Water Sorption, Density, and Fractional Free Volume of Pebax and MWNT-Pebax Membranes

membrane	degree of swelling in water	density (g/cm ³)	FFV (%)
Pebax-1657	2.4	1.157	2.6
2% MWNT-Pebax	4.3	1.102	7.2
5% MWNT-Pebax	9.6	1.049	11.7

groups. Thus, v_w in cubic centimeters/gram was 0.6475. The density of the membrane depends upon the concentration of MWNT in the polymer. Table 2 shows density data for neat and nanocomposite membranes.

To determine the interactive groups (IEC) remaining in the cross-linked polymer, the membranes were soaked in 50 mL of 0.01 N sodium hydroxide solution for 12 h at ambient temperature. Then, 10 mL of solution was titrated against 0.01 N sulfuric acid. The sample was regenerated with 1 M hydrochloric acid, washed free of acid with water, and dried to a constant weight. The IEC was calculated according to the equation:³³

$$\text{IEC} = \frac{(B - P)(0.01)(5)}{m}$$

where B is the amount of 0.01 N sulfuric acid used to neutralize the blank sample, P is the amount of 0.01 N sulfuric acid used to neutralize the membranes, 0.01 is the factor used to account for normality of sulfuric acid/NaOH, and 5 is the factor corresponding to the ratio of the amount of NaOH taken to dissolve the polymer to the amount used for titration, and m is sample mass in grams.

The extent of swelling of the uncross-linked Pebax membranes with and without MWNT was determined by a sorption study in water. Preweighed strips of neat, MWNT loaded, and cross-linked membranes (2 cm diameter) were immersed in pure water at 30 °C. The films were taken out after different soaking periods and quickly weighed after carefully wiping out excess liquid to monitor the mass increase of the membranes to determine the amount absorbed at the particular time " t ". The films were then quickly placed back in water. The process was repeated until the films attained steady state as indicated by constant weight after a certain period of soaking time. The degree of swelling was determined from³³

$$\text{degree of swelling} = \frac{M_s}{M_d}$$

where M_s = mass of the swollen polymer in grams and M_d = mass of the dry polymer in grams.

2.4. Gas Permeability Studies. A schematic diagram of the experimental setup is shown in Figure 2. The gas permeation tests were conducted using an indigenously designed and fabricated permeation test cell made of stainless steel 316. Gas inlet and outlet ports were provided in the test cell for the transport of feed, permeate, and retentate streams. The test cell contained a circular perforated plate affixed with a mesh to support a membrane of effective area 42 cm². Neoprene rubber "O" ring and vacuum grease were used to provide a leak-tight arrangement. Feed, permeate, and retentate lines were made of 1/4 in. stainless steel (SS) 316 tubes. Nut and ferrule compression fittings were used in the manifold to transport the gas streams. The vacuum line consisted of a network of high-vacuum rubber and glass valve connections capable of providing a pressure of ≤ 0.5 mmHg. Needle valves (Swagelok) with 1/4 in. SS 316 end connections were used to regulate the flow of

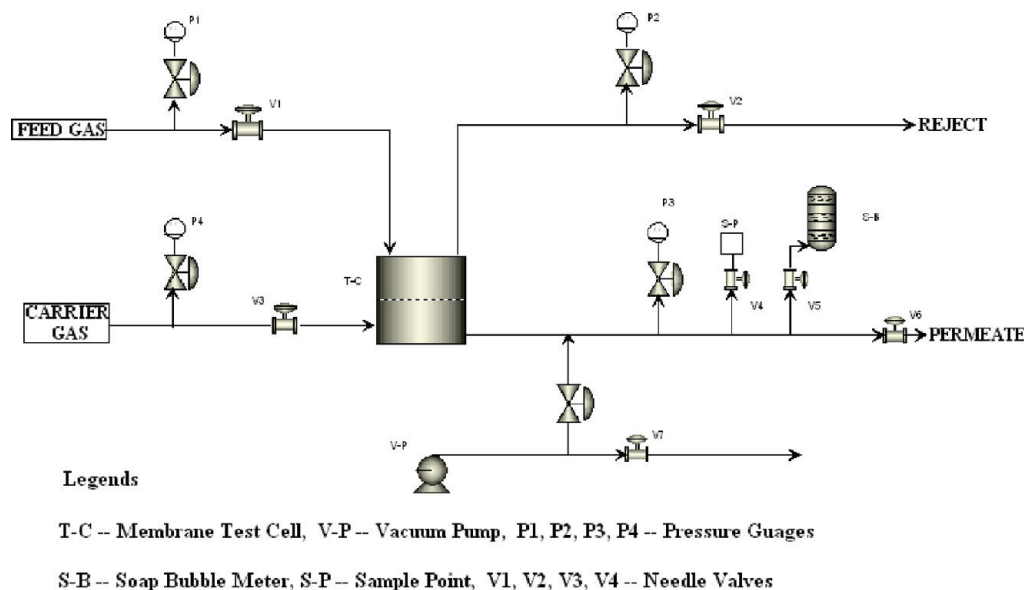


Figure 2. Schematic of a high-pressure gas permeability manifold.

inlet and outlet streams. The experimental manifold was flexible for studies with both pure gases and mixtures.

In the present work, all the experiments were conducted with pure H_2 , O_2 , N_2 , and CO_2 gases. Since pure gases were used as the feed, the permeate flow was directly measured without employing a carrier gas. Before each experiment the permeate line was evacuated with a vacuum pump (Hindhivac, Bangalore, India) with the perforated plate support ensuring no membrane rupture. The feed and retentate lines cannot be evacuated and hence were flushed with the feed to remove residual air and ensure maximum purity of the gas inside the cell. Experiments were conducted over a feed pressure range of 1.0–3.0 MPa at ambient temperature ($30 \pm 2^\circ C$). Feed gas was introduced slowly into the upper chamber of the test cell by means of a needle valve with the outlet valve kept partially closed until the gauge indicated the desired pressure. Continuous flow of the gas in the feed chamber was maintained. Once steady state was attained the flow rate of permeate was measured with the help of a soap bubble meter. Data were recorded until a consistent permeation rate was obtained. Since it is difficult to accurately determine the exact thickness of the skin layer of a composite membrane, the authors carefully peeled off the Pebax top layer from the PES substrates in order to measure the effective thickness for permeability calculation. The thickness was found to vary between 15 and 20 μm after which the permeability coefficient (K) was determined from

$$K = \frac{Q\delta}{tA(p_1 - p_2)}$$

where Q is the volume of permeated gas (cubic centimeters (standard temperature and pressure (STP))), δ is the effective membrane thickness (centimeters), t is the permeation time (seconds), A is the effective membrane area (centimeters squared) for gas permeation, and p_1 and p_2 are the feed side and permeate side partial pressures (centimeters of Hg), respectively. The unit of permeability is denoted in barrers [1 barrer = 10^{-10} (cm^3 (STP) cm/cm^2 s $cmHg$)]. The authors also prepared free-standing MWNT-Pebax nanocomposite membranes of 20 μm thickness to verify the permeability obtained with the PES supported membranes and the results were found to be comparable. The permeability through the PES supported

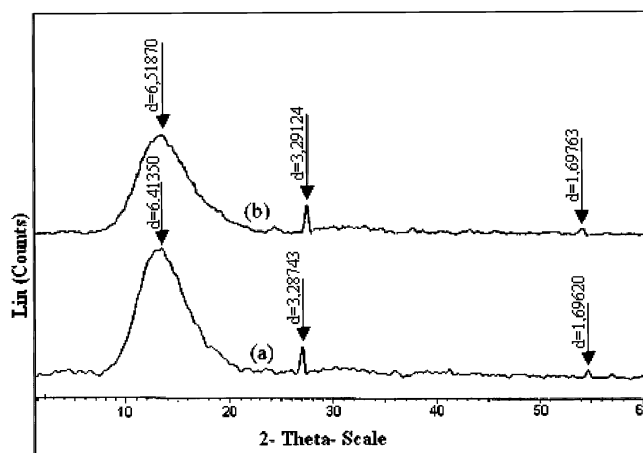


Figure 3. XRD of (a) Pebax and (b) 2% MWNT-Pebax membranes.

membranes are reported in this study as such membranes provide a pathway for scale-up and commercial exploitation. The selectivity (α) is defined as the pure gas permeability ratio of faster gas to that of the slower gas.

$$\alpha = \frac{K_a}{K_b}$$

3. Results and Discussion

3.1. Membrane Characterization. 3.1.1. WAXD. Among the different degrees of loading investigated, a 2% MWNT loaded membrane was chosen for comparison with the pristine polymer as it exhibited high selectivity. Wide-angle X-ray diffractograms of Pebax and 2% MWNT-Pebax composite are shown in Figure 3. Both membranes exhibit semicrystalline nature. Pebax (diffractogram a) is a semicrystalline polymer which shows narrow diffraction peaks at 12° , 26° , and 54° of 2θ . The corresponding XRD peaks obtained for Pebax nanocomposite (diffractogram b) undergo a slight shift toward the right side and are marginally broader as indicated in the figure which reveals an increase from 6.413 to 6.518, 3.287 to 3.291, and 1.696 to 1.697, respectively. This indicates a marginal increase in intersegmental spacing which may lead to enhancement of an amorphous nature and polymer permeability.

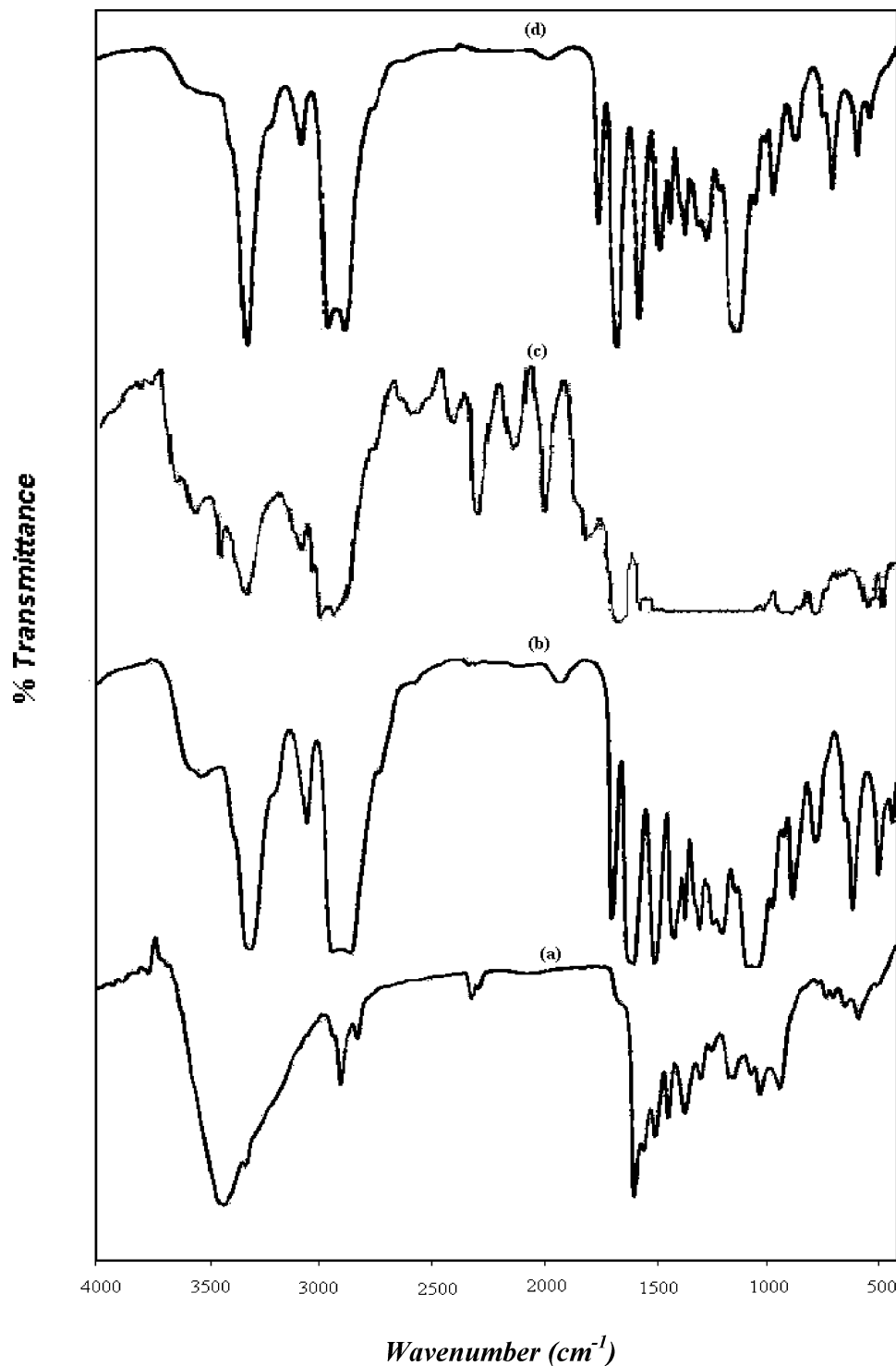


Figure 4. FTIR of (a) MWNT, (b) Pebax, (c) cross-linked Pebax, and (d) 2% MWNT-Pebax membranes.

3.1.2. FTIR. Figure 4a represents FTIR spectra of MWNT. The characteristic peak at 1652 cm^{-1} represents the presence of a C=C bond. In neat Pebax (Figure 4b), the characteristic peaks at 1732 and 1102 cm^{-1} represent C=O and C-O stretching vibrations, respectively. Two more peaks at 1641 and 3300 cm^{-1} indicate the presence of H-N-C=O and the N-H group, respectively. The stretching vibration at 2940 cm^{-1} indicates the presence of aliphatic C-H . The C=O stretching in the amide group of Pebax is constituted of two types, the free amide C=O peak at 1657 cm^{-1} and the hydrogen bonded amide peak at 1640 cm^{-1} . The spectra of cross-linked Pebax is

shown in Figure 4c, wherein the peak at 1545 cm^{-1} corresponding to the C-O stretching band has reduced due to urethane linkage between terminal -OH groups of Pebax and carbonyl groups of the TDI cross-linker. The emergence of new peaks at 1645 cm^{-1} is attributed to the formation of urea type linkages during the interaction between the reactive -NH groups of Pebax and TDI. FTIR spectra of 2% MWNT-Pebax represented by Figure 4d reveals increased absorbance and shift of the peak at 1650 cm^{-1} , which means that the MWNT interacts mainly with the -NH group present in the amide block of the block copolymer. The steepness of the peak at 1641 cm^{-1} may

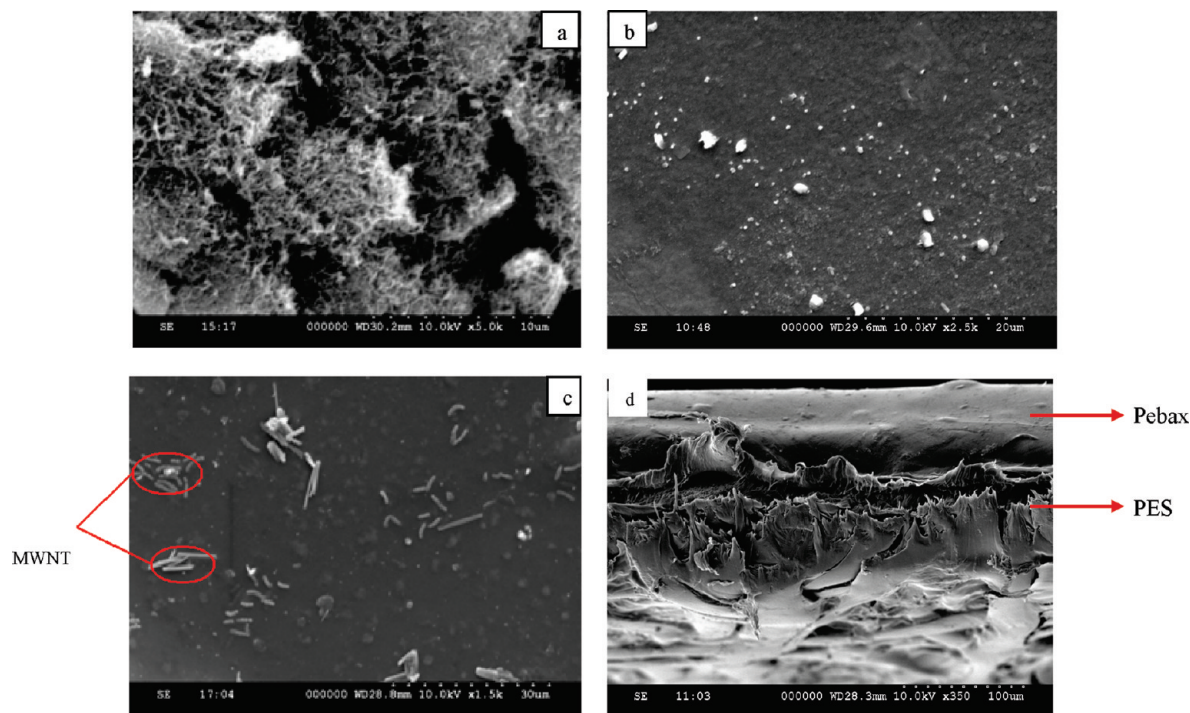


Figure 5. SEM pictures representing the (a) morphology of multiwalled carbon nanotubes, (b) surface of neat Pebax membrane, (c) surface of 2% MWNT loaded Pebax membrane, and (d) cross-section of a neat Pebax membrane.

Table 3. Effect of MWNT Concentration on Permeability of Neat and Crosslinked Pebax Membranes at 1 MPa Feed Pressure

% MWNT	membrane thickness (μm)	permeability (barrer ^a)							
		H ₂		CO ₂		O ₂		N ₂	
		Pebax	X-Pebax	Pebax	X-Pebax	Pebax	X-Pebax	Pebax	X-Pebax
0	15	32.11	5.83	55.85	13.38	4.69	1.19	1.39	0.24
2	15	35.82	2.51	329.74	3.54	8.61	0.22	4.20	0.03
5	20	40.96	7.18	262.15	17.47	12.03	1.05	4.48	0.21

^a 1 barrer = 10^{-10} [cc(STP) cm]/[cm² s cmHg].

be due to the combined effect of C=C and C=O groups. Thus, MWNT has chemical interactions with the Pebax membrane and is not merely physically present.

3.1.3. SEM. The morphology of MWNT, Pebax, and MWNT-Pebax were investigated using scanning electron microscopy (SEM). The morphology of the MWNT is shown in Figure 5a. The MWNT are present as a continuous network in the form of “ropes” and form lump like agglomerates, which are held together by van der Waal’s forces. Parts b and c of Figure 5 exhibit the surface morphologies of neat and 2% MWNT loaded Pebax membranes, respectively. Neat Pebax shows a clear and homogeneous surface whereas the nanocomposite shows the MWNT to be dispersed randomly in the form of agglomerates. Figure 5d represents a cross-sectional view of neat Pebax that exhibits the two layers of the thin film composite membrane comprised of a Pebax top layer having smooth horizontal morphology and a PES substrate layer which is ultraporous (indicated in the figure).

3.1.4. IEC, Water Sorption, Density, and FFV. The ion exchange capacity of neat Pebax membrane was found to be 5.32 meq/g whereas that of the cross-linked membrane (without MWNT) reduced to 3.12 meq/g, which means that approximately 41.4% of the reactive functional groups of the polymer were cross-linked by TDI. The 2% MWNT loaded membrane with the same degree of cross-linking revealed an IEC value of 3.47 meq/g that is marginally higher than its cross-linked version, which meant that MWNTs, which exhibited an IEC value of 9.5 meq/g in the pure state, contribute to the reactive

nature of the composite and possess the ability to interact with the polymer matrix, which supports FTIR interpretation.

Table 2 shows that the density of the uncross-linked Pebax membranes reduced from 1.157 to 1.049 g/cm³ even as the MWNT concentration was varied from 0 to 5%. The corresponding FFV increased from 2.6% to 11.7% indicating that MWNT loading could induce the presence of microvoids within the polymer matrix making it more permeable. The calculations have revealed that a small concentration of 5% wt MWNT could enhance the free volume of the composite membrane to 4.5 times that of the neat membrane. Table 2 also displays sorption data that exhibit an increase in the degree of swelling from 2.4 for neat Pebax to 4.3 for 2% loading and 9.6 for 5% MWNT concentration which substantiates FFV calculations. After 2 days of soaking in water, the MWNT underwent an increase in weight from 0.0007 g to a final constant weight of 0.0066 g indicating a degree of swelling of 9.4, which meant that MWNT would contribute to water sorption and therefore void volume as well.

3.2. Permeability Results. 3.2.1. Effect of MWNT Incorporation. Tables 3 and 4 exhibit the effect of MWNT concentration to the extent of 2% and 5% of the polymer weight on the gas permeation characteristics of Pebax and X-Pebax membranes at 1 MPa constant feed pressure. In general, the permeability of the gases was found to be in the order CO₂ > H₂ > O₂ > N₂. CO₂ has greater solubility in Pebax polymer which is more or less inert to the other gases. The kinetic diameter of CO₂ (3.3 Å) is also smaller than those of O₂ (3.46 Å) and N₂ (3.64 Å), leading to greater diffusivity compared to

Table 4. Selectivity of Neat and Crosslinked Pebax Membranes for Varying MWNT Concentration at 1 MPa Feed Pressure

% MWNT	selectivity							
	H ₂ /N ₂		O ₂ /N ₂		CO ₂ /N ₂		CO ₂ /H ₂	
	Pebax	X-Pebax	Pebax	X-Pebax	Pebax	X-Pebax	Pebax	X-Pebax
0	23.1	24.8	3.4	5.1	40.2	56.9	1.7	2.3
2	8.5	82.5	2.1	7.1	78.6	83.2	9.2	1.4
5	9.1	34.7	2.7	5.1	58.5	84.5	6.4	2.4

the two gases that constitute air. As observed from Table 3, cross-linking with TDI (X-Pebax) considerably decreased the permeability. TDI could possibly form urea type linkages with the more reactive amide groups and urethane linkages with the terminal hydroxyl groups of Pebax causing the polymer to become more compact. X-Pebax consistently exhibited lower permeability but greater selectivity (pure gas permeability ratio) than neat Pebax as shown in Table 4.

After MWNT loading, the uncross-linked Pebax membranes showed a substantial enhancement in permeability for all the gases. Especially, CO₂ molecules appeared to experience greater solubility and exhibited a more substantial increase from 55.8 barrers at 0% MWNT to 262.1 barrers at 5% loading. A decrease in H₂/N₂ and O₂/N₂ selectivities was observed in contrast to the CO₂/N₂ gas pair for which selectivity increased from 40.2 to 58.5. This meant that the MWNTs could have affinity for the quadrupolar CO₂ gas compared to the relatively inert H₂, O₂, and N₂ gases. X-Pebax membranes incorporated with MWNT exhibited a rise in selectivity without considerable reduction in permeability. A moderate selectivity of 7.1 was observed for the O₂/N₂ system with 2% MWNT-X-Pebax membrane. Thus, cross-linking induced lower permeability and higher selectivity. However, the permselectivity of X-Pebax membranes could be improved through MWNT incorporation.

Interestingly, the Pebax membranes were more permeable to CO₂ than even hydrogen, which is generally the faster permeating gas through most glassy polymers due to its smaller molecular size and kinetic diameter of 2.89 Å. The quadrupolar nature of CO₂ combined with the rubbery nature of Pebax renders it more permeable than H₂.³⁴ The poor solubility of N₂, which would be the most inert among all the gases tested, combined with its slow diffusivity resulting from the larger kinetic diameter (3.64 Å) contribute to its low permeability.

3.2.2. Effect of Feed Pressure. The 2% MWNT loading was chosen to further investigate the effect of feed pressure, which was varied from 1.0 to 3.0 MPa in intervals of 0.5 MPa each. The results are compared with neat Pebax membrane in Figures

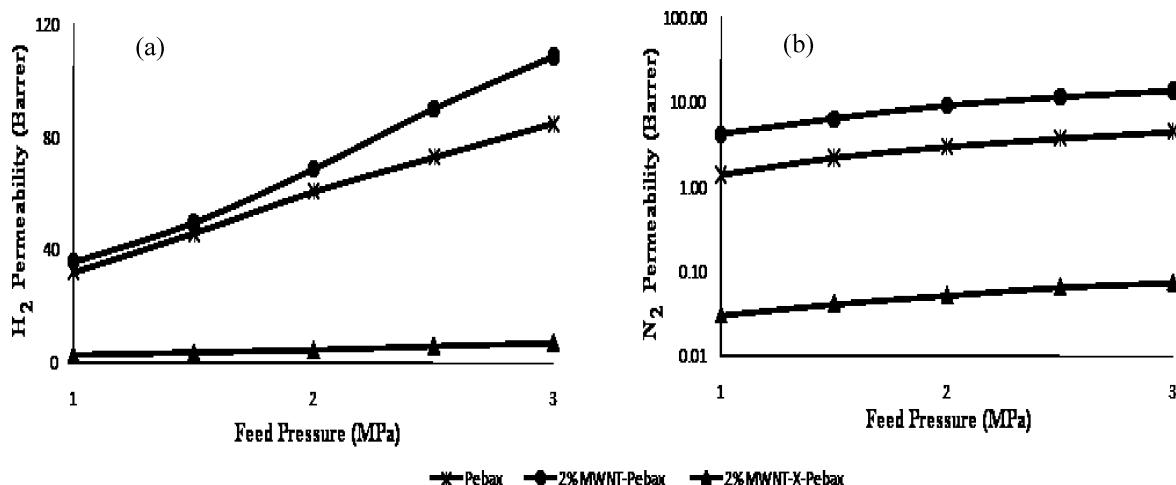
6–9. The permeability of all the gases increased with pressure for all the membranes as shown in Figures 6 and 7 due to increasing solubility and the driving force for mass transfer. For neat Pebax, CO₂ permeability increased from 55.8 to 183.8 barrers whereas that of H₂ was enhanced from 32.1 to 84.9 barrers. The comparatively higher CO₂ permeability appears to stem from increasing carbon dioxide solubility attributed to strong affinity of the polar ether linkages of Pebax for this particular gas.³⁴

In case of the uncross-linked nanocomposite, a decrease in selectivity with respect to the relatively inert O₂/N₂ and H₂/N₂ systems can be observed in Figure 8. Pebax has both rubbery polyether domains and glassy polyamide domains with most of the gas transport occurring through the rubbery domains. Sorption contribution of the glassy domain is negligible due to a combination of high crystallinity of such domains and the higher proportion of rubbery domains available in Pebax polymer.³⁵

The cross-linked nanocomposite was the least permeable but in general the most selective. Cross-linking increases the cohesive energy density of the membrane and size-selective nature but reduces flux. CO₂/N₂ selectivity increased from 83.2 to 162 in the pressure range of 1–3 MPa. The rise in ideal selectivity of CO₂ with respect to both N₂ and H₂ gases could be attributed to plasticization of the polymer matrix by carbon dioxide with increasing pressure (Figure 9). The weak size-sieving ability of the rubbery polyether phase also contributes to CO₂ selectivity.³⁵ The corresponding increase for the H₂/N₂ system was 82.5–90. Though selectivity for the O₂/N₂ gas pair reduced marginally from 7.1 to 6.8, these values show potential for air separation (Figure 8).

4. Conclusions

Pebax-1657 was used as a base polymer for physicochemical modification through incorporation of MWNT and cross-linking by TDI. The percentage of MWNT loading was varied to study

**Figure 6.** Effect of feed pressure on permeabilities of (a) H₂ and (b) N₂ gases.

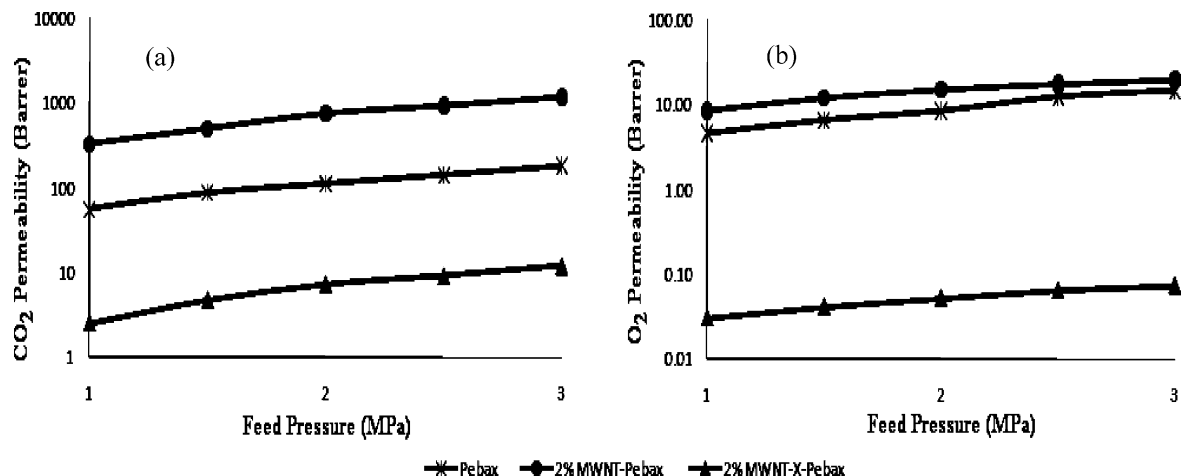


Figure 7. Effect of feed pressure on permeabilities of (a) CO₂ and (b) O₂ gases.

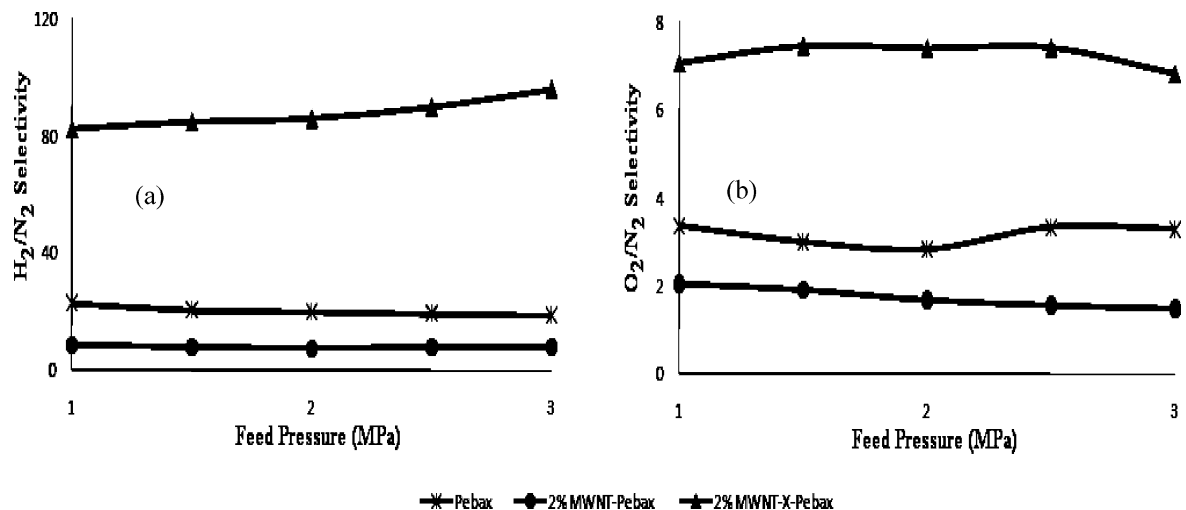


Figure 8. Variation of selectivities of (a) H₂/N₂ and (b) O₂/N₂ systems with feed pressure.

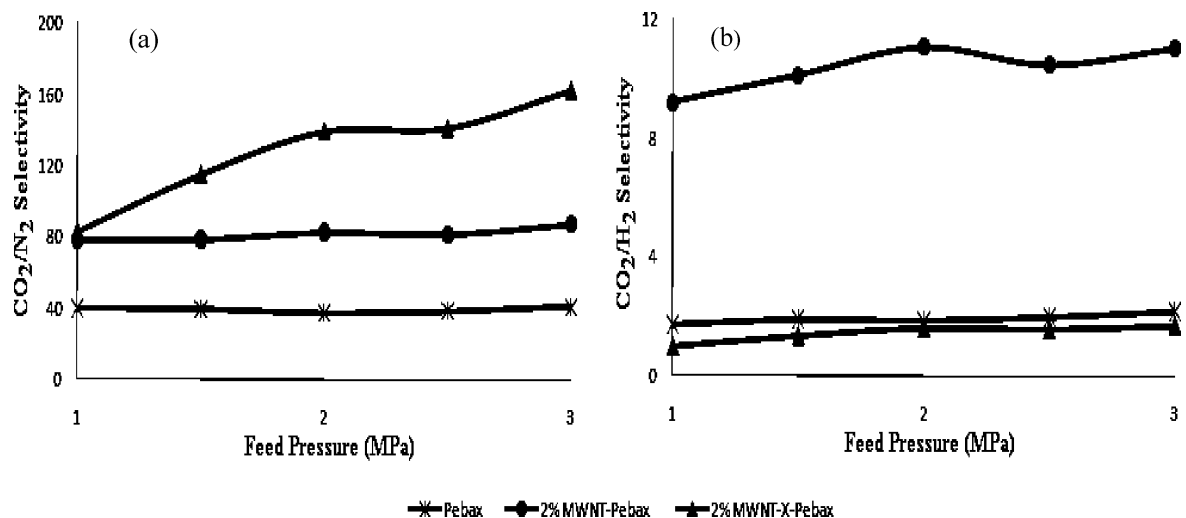


Figure 9. Variation of selectivities of (a) CO₂/N₂ and (b) CO₂/H₂ systems with feed pressure.

the permeation of pure H₂, N₂, O₂, and CO₂ gases. Characterization by XRD and FTIR showed nanotubes to induce both physical changes and chemical interactions within the matrix. SEM revealed bundled and randomly oriented dispersion of nanotubes. Incorporation of MWNT caused an increase in free volume as revealed by FFV calculations and water sorption studies. The ion exchange capacity of the polymer was found

to reduce after cross-linking with TDI. It appears that the trade-off between flux and selectivity could be optimized by controlling the concentration of MWNT in cross-linked Pebax membranes. The 2% MWNT-X-Pebax exhibited potential for gas separation applications due to high selectivities obtained for CO₂/N₂ and H₂/N₂ systems. Performance for O₂/N₂ was also reasonable. CO₂ solubility and permeability in this block

copolymer is high and gets enhanced with increasing pressure due to plasticization. The MWNT loaded uncross-linked membranes exhibited high flux with low selectivity. However, after cross-linking it showed potential for separation applications in power plants, ammonia production industry, welding and medical applications, besides the water-gas shift reaction due to enhancement in selectivities. Thus, incorporation of selective inorganic fillers such as MWNT into gas separating polymer membranes could improve their commercial viability. Though selectivities may decrease in the case of binary or multicomponent mixtures due to coupling effect, the MWNT loaded X-Pebax membrane has shown enough potential for further research.

Acknowledgment

The first author R. Surya Murali is grateful to the Council of Scientific and Industrial Research (CSIR), New Delhi, India, for funding his Ph.D. research programme under the GATE-JRF scheme.

Literature Cited

- (1) Koros, W. J.; Mahajan, R. Pushing the limits on possibilities for large scale gas separation: which strategies. *J. Membr. Sci.* **2000**, *175*, 181–196.
- (2) Stern, S. A. Polymers for Gas Separations: The Next Decade. *J. Membr. Sci.* **1994**, *94*, 1–65.
- (3) Maier, G. Gas Separation with Polymer Membrane. *Angew. Chem., Int. Ed.* **1998**, *37*, 2960–2974.
- (4) Robeson, L. M. Correlation of Separation Factor versus Permeability for Polymeric Membranes. *J. Membr. Sci.* **1991**, *62*, 165–185.
- (5) Kim, S.; Pechar, T. W.; Marand, E. Poly(imide siloxane) and Carbon Nanotube Mixed Matrix Membranes for Gas Separation. *Desalination* **2006**, *192*, 330–339.
- (6) Merkel, T. C.; He, Z.; Pinnau, I.; Freeman, B. D.; Meakin, P.; Hill, A. J. Effect of Nanoparticles on Gas Sorption and Transport in Poly(1-trimethylsilyl-1-propyne). *Macromolecules* **2003**, *36*, 6844–6855.
- (7) He, Z.; Pinnau, I.; Morisato, A. Nanostructured Poly(4-methyl-2-pentynyl)/Silica Hybrid Membranes for Gas Separation. *Desalination* **2002**, *146*, 11–15.
- (8) Pinnau, I.; He, Z. Filled Superglassy Membrane. U.S. Patent 6,316,684, November 13, 2001.
- (9) Merkel, T. C. Organic-Inorganic Nanocomposite Membranes for Vapor Separations. Ph.D. Dissertation, North Carolina State University, Raleigh, NC, 2001.
- (10) Sadeghi, M.; Khanbabaei, G.; Dehaghani, A. H. S.; Sadeghi, M.; Aravand, M. A.; Akbarzade, M.; Khatti, S. Gas Permeation Properties of Ethylene Vinyl Acetate-Silica Nanocomposite Membranes. *J. Membr. Sci.* **2008**, *322*, 423–428.
- (11) Ekiner, O. M.; Simmons, J. W. Gas Separation Membranes made from Blends of Aromatic Polyamide, Polyimide or Polyamide-imide Polymers. U.S. Patent 5,248,319, September 28, 1993.
- (12) Cai, Y.; Wang, Z.; Yi, C.; Bai, Y.; Wang, J.; Wang, S. Gas Transport Property of Polyallylamine-poly(vinyl alcohol)/Polysulfone Composite Membranes. *J. Membr. Sci.* **2008**, *310*, 184–196.
- (13) Deng, J.; Zhang, X.; Wang, K.; Zou, H.; Zhang, Q.; Fu, Q. Synthesis and Properties of Poly(ether urethane) Membranes Filled with Isophorone diisocyanate-grafted Carbon Nanotubes. *J. Membr. Sci.* **2007**, *288*, 261–267.
- (14) Yave, W.; Car, A.; Peinemann, K. V.; Shaikh, M. Q.; Rätzke, K.; Faupel, F. Gas Permeability and Free Volume in Poly(amide-b-ethylene oxide)/Polyethylene Glycol Blend Membranes. *J. Membr. Sci.* **2009**, *339*, 177–183.
- (15) Joseph, R.; Flesher, J. R. PEBA Polyether Block Amide-A New Family of Engineering Thermoplastic Elastomers. In *High Performance Polymers: Their Origins and Development*; Seymour, R. B., Kirshenbaum, G. S., Eds.; Elsevier: New York, 1986; p 401.
- (16) *PEBAX-Basis of Performance, Polyether Block Amide*, Elf Atochem Technical Document, Paris, France.
- (17) Tocci, E.; Gugliuzza, A.; Lorenzo, L. D.; Macchione, M.; Luca, G. D.; Drioli, E. Transport Properties of a Co-poly(amide-12-b-ethylene oxide) membrane: A Comparative Study Between Experimental and Molecular Modeling Results. *J. Membr. Sci.* **2008**, *323*, 316–327.
- (18) Potreck, J.; Nijmeijer, K.; Kosinski, T.; Wessling, M. Mixed Water Vapour/Gas Transport through the Rubbery Polymer PEBAX-1074. *J. Membr. Sci.* **2009**, *338*, 11–16.
- (19) Liu, L.; Chakma, A.; Feng, X. Propylene Separation from Nitrogen by Poly(ether block amide) Composite Membranes. *J. Membr. Sci.* **2006**, *279*, 645–654.
- (20) Cong, H.; Zhang, J.; Radosz, M.; Shen, Y. Carbon Nanotube Composite Membranes of Brominated Poly(2,6-diphenyl-1,4-phenylene oxide) for Gas Separation. *J. Membr. Sci.* **2007**, *294*, 178–185.
- (21) Andrews, R.; Weisenberger, M. C. Carbon Nanotube Polymer Composites. *Curr. Opin. Solid State Mater. Sci.* **2004**, *8*, 31–37.
- (22) Ounaies, Z.; Park, C.; Wise, K. E.; Siochi, E. J.; Harrison, J. S. Electrical Properties of Single Wall Carbon Nanotube Reinforced Polyimide Composites. *Compos. Sci. Technol.* **2003**, *63*, 1637–1646.
- (23) Dalton, A. B.; Collins, S.; Munoz, E.; Razal, J. M.; Ebron, V. H.; Ferraris, J. P.; Coleman, J. N.; Kim, B. G.; Baughman, R. H. Super-Tough Carbon-Nanotube Fibres. *Nature* **2003**, *423*, 703.
- (24) Coleman, J. N.; Blau, W. J.; Dalton, A. B.; Munoz, E.; Collins, S.; Kim, B. G.; Razal, J. M.; Selvidge, M.; Vieiro, G.; Baughman, R. H. Improving the Mechanical Properties of Single-Walled Carbon Nanotube Sheets by Intercalation of Polymeric Adhesives. *Appl. Phys. Lett.* **2003**, *82*, 1682–1684.
- (25) Sharma, A.; Kumar, S.; Tripathi, B.; Singh, M.; Vijay, Y. K. Aligned CNT/Polymer Nanocomposite Membranes for Hydrogen Separation. *Int. J. Hyd. Energy* **2009**, *34*, 3977–3982.
- (26) Hinds, B. J.; Chopra, N.; Rantell, T.; Andrews, R.; Gavalas, V.; Bachas, L. G. Aligned Multiwalled Carbon Nanotube Membranes. *Science* **2004**, *303*, 62–65.
- (27) Sridhar, S.; Suryamurali, R.; Smitha, B.; Aminabhavi, T. M. Development of Crosslinked Poly (ether-block-amide) Membrane for CO₂/CH₄ Separation. *Colloids Surf., A: Physicochem. Eng. Aspects* **2007**, *297*, 267–274.
- (28) Li, C.; Shao, H.; Zhong, S. Preparation Technology of Organic-Inorganic Hybrid Membrane. *Huaxue Jinzhan* **2003**, *16*, 83–89.
- (29) Lozano, A. E.; de la Campa, J. G.; de Abajo, J.; Espeso, J. Effect of Substituents on the Permeation Properties of Polyamide Membranes. *J. Membr. Sci.* **2006**, *280*, 659–665.
- (30) Sakaguchi, T.; Nojiri, D.; Hashimoto, T. Gas Permeation Properties of Poly(2,5-dialkyl-p-phenyleneethynylene) Membranes. *Polym. Bull.* **2008**, *60*, 271–279.
- (31) Bondi, A. *Physical Properties of Molecular Crystals, Liquids and Glasses*; Wiley: New York, 1968.
- (32) van Krevelen, D. W. *Properties of Polymers: Their Correlation with Chemical Structure*, 3rd ed.; Elsevier: Amsterdam, The Netherlands, 1990.
- (33) Smitha, B.; Sridhar, S.; Khan, A. A. Polyelectrolyte Complexes of Chitosan and Poly(acrylic acid) as Proton Exchange Membranes for Fuel Cells. *Macromolecules* **2004**, *37*, 2233–2239.
- (34) Bondar, V. I.; Freeman, B. D.; Pinnau, I. Gas Sorption and Characterization of Poly(ether-b-amide) Segmented Block Copolymers. *J. Polym. Sci., Part B: Polym. Phys.* **1999**, *37*, 2463–2475.
- (35) Bondar, V. I.; Freeman, B. D.; Pinnau, I. Gas Transport Properties of Poly(ether-b-amide) Segmented Block Copolymers. *J. Polym. Sci., Part B: Polym. Phys.* **2000**, *38*, 2051–2062.

Received for review October 23, 2009

Revised manuscript received May 20, 2010

Accepted June 4, 2010

IE9016495